Acta Polytechnica **63**(1):1–10, 2023
https://doi.org/10.14311/AP.2023.63.0001
© 2023 The Author(s). Licensed under a CC-BY 4.0 licence
Published by the Czech Technical University in Prague

INDUCTION MOTOR MECHANICAL DEFECT DIAGNOSIS USING DWT UNDER DIFFERENT LOADING LEVELS

Ahcene Bouzida[a,*], Radia Abdelli[b], Aimad Boudouda[c]

[a] *University of Bouira, Faculty of Sciences and Applied Sciences, Department of Electrical Engineering, 10000, Bouira, Algeria*

[b] *University of Bejaia, Faculty of Technology, Department of Electrical Engineering, 06000, Bejaia, Algeria*

[c] *University of Boumerdes, Faculty of Technology, Laboratoire Ingénierie des Systèmes et Télécommunications (LIST), 35000, Boumerdes, Algeria*

[*] corresponding author: a.bouzida@univ-bouira.dz

Abstract. The information extraction capability of the widely used signal processing tool, FFT for diagnosing induction machines, is commonly used at a constant load or at different levels. The loading level is a major influencing factor in the diagnostic process when the coupled load and the machine come with natural mechanical imperfections, and at a low load, the mechanical faults harmonics are strongly influenced. In this context, the main objective of this work is the detection of the mechanical faults and the study of the effect of the loading level on the induction motor diagnostic process. We have employed a diagnosis method based on discrete wavelet transform (DWT) for the multi-level decomposition of stator current and extracting the fault's energy stored over a wide frequency range. The proposed approach has been experimentally tested on a faulty machine with dynamic eccentricity and a shaft misalignment for three loading levels. The proposed method is experimentally tested and the results are provided to verify the effectiveness of the fault detection and to point out the importance of the coupled load.

Keywords: Induction motor, fault diagnosis, eccentricity, misalignment, DWT, energy, loading levels.

1. Introduction

Incorrect configuration of the electrical circuit and mechanical faults in industrial induction machines can lead to serious economic losses, as well as other losses in less tangible terms. If the stator or rotor are incorrectly diagnosed and interpreted as faulty (wrong diagnostic decision), there will be important costs added from the unnecessary maintenance operation, disassembly of the motor, or from a false positive decision which leads to a halt of the entire production process. In addition, the credibility and the efficiency of maintenance operations and technicians can be seriously compromised. In the opposite case, if the machine is identified as healthy (false negative), the fault can aggravate and an accelerate the degradation of the machine and the coupled load may occur. This degraded operation can result in even higher economic costs, the consequences of unplanned shutdowns of production, risks to the safety of users and damage to the company's reputation. These consequences resulting from an incorrect diagnosis of the state of the machine are not at all negligible, at least when using the techniques commonly used in the industry.

The most frequently used methods of diagnosis of mechanical and electrical defects in the industry are derived from the technique of Motor Current Signature Analysis (MCSA) when the defects are classified as electrical faults and can be easily detected by analysing the electrical signature [1–4]. This technique is often used to analyse the stator current, vibration, or torque acquired during operation using the Fast Fourier Transform (FFT). The principle of this method is based on the evaluation of the amplitudes of a predefined frequency component linked to faults. In general, induction machines have two ranges of frequencies that can be affected by faults, the first one is located in the low frequency band and the second one in the high band. Therefore, the tracking of these components without a constant load and mixed faults makes the diagnostic process very difficult and prone to errors. Otherwise, the diagnosis at the low loading level is different from the higher loading level because of the variation of fault harmonics with slip and the amplitude of space harmonics. For a diagnosis of mechanical faults, such as rotor asymmetries, load oscillations, and misalignments using the lower sideband harmonic (LSH) based approach, it is difficult to decide whether the machine is in a fault condition or not [5–7].

The presence of various phenomena in induction motors, such as load torque oscillations and voltage fluctuations, make the diagnostic process notably difficult [8–10]. Despite the prevalence of this circumstance, however, researchers have rarely probed the correlation between the presence of these phenomena and the defect in the machine. Mills, compressors, and other machines that introduce torque oscillations often use induction motors with a degree of eccentricity or even with misalignment [8]. In these instances,

the implementation of the classical FFT method imposes significant limits; the frequencies induced by load torque fluctuations and level may be identical to fault-related frequencies and magnitudes [11], resulting in a wrong diagnostic decision. The similarities between the FFT spectra of a faulty motor and the same motor in a healthy condition but operated under high load and oscillating load torque can result in such a wrong decision. The obvious similarity in spectral analysis could lead to an inaccurate diagnosis. Due to these disadvantages, alternate approaches to diagnosis based on techniques, such as the Discrete Wavelet Transform (DWT) for the analysis of the stator current under wide frequency band, becomes acceptable in this situation [12, 13]. A proposed works in [14, 15], present an effective machine-learning-based fault diagnosis method, developed for induction motors driven by variable frequency drives (VFDs). Two identical induction motors under healthy, single, and multi-fault conditions were tested in the lab. A Signal processing technique, the discrete wavelet transform, is chosen to extract features for machine learning. The derived DWT diagnosis method is proposed to detect and locate the insulated gate bipolar translator open-circuit fault. The discrete wavelet transform is used as a pre-treatment technique for three-phase output currents. Euclidean distance between every two of the energy vectors are calculated for measuring the current similarity [16].

In this study, we present a technique for diagnosing mechanical faults in induction machines. The method is contrasted with the standard decomposition in multi-levels via DWT of the stator current in a steady state, and additional steps are required to determine the energy associated with each level of decomposition [12, 13]. The proposed energy estimation is used to analyse stator currents when the spectral content is distributed over a wide frequency band. To validate this method, several experiments, including those with a healthy machine, an eccentric machine, and shaft misalignment, are carried out to simulate a variety of failure scenarios and operating settings. The focus of this study is on selecting the appropriate decomposition levels for information extraction corresponding to faults caused by stator currents. We will try to show how the harmonic content caused by mechanical faults is largely influenced by the loading level. A dynamic eccentricity fault of 50 % and a shaft misalignment fault will be discussed and validated using this technique.

2. Wavelet decomposition and energy extraction

The Wavelet Transform WT provides time tracking of frequency harmonics of a continuous temporal signal, the main analysing functions are called wavelets. These functions vary their time-scale coefficients to their frequency to be very narrow at higher frequency and broader at a lower frequency. WT is a powerful means for analysing stationary and transient currents, voltages, and vibration in order to detect the presence of failure. DWT is the discrete version of WT and the most common transform employed in electrical engineering applications, particularly in monitoring systems for detection, localisation, and classification of the power system perturbations in time and frequency domains [13, 17, 18].

The DWT has become an effective tool in digital signal processing. It can be written in the same form as the continuous version, which highlights the close relationship between the continuous and the discrete version of this transform. The DWT is based on a discrete scale and localisation parameters that are power of two (2). The values of dilation and translation factors s and τ are: $s = 2j$, $\tau = k * 2^j$ and $(j, k) \in Z$, respectively. These proprieties are achieved by using a scaling function ϕ that is a wavelet aggregate at scales larger than 1. When the functions $\hat{\psi}(\omega)$ and $\hat{\varphi}(\omega)$ are the Fourier transforms of $\psi(\omega)$ and $\varphi(\omega)$, respectively, it leads to high-frequency resolutions at low frequencies and high-time resolutions at high frequencies, and eliminating the redundant information. The positive frequency, contains information in the interval $[0, \pi]$, and contains information in the interval $[\pi, 2\pi]$. Therefore, the two functions have a complete spectral content of the analysed signal without any overlapping, redundancy, or loss. Two filters, $h(n)$ and $g(n)$, are obtained by the inner product of $(\phi(t), \varphi(t))$ allowing the decomposition of the entire signal into $[0, \pi]$. The filters are given by [19–24]:

$$\begin{cases} h(n) = \left\langle 2^{-l}\phi(2^{-l}t)\phi(t-n)\right\rangle \\ g(n) = \left\langle 2^{-j}\psi(2^{-j}t)\psi(t-n)\right\rangle \end{cases} ., \; j = 0, 1, ... \quad (1)$$

For the purpose of decomposing the signal across the entire allowed frequency range, a mother wavelet can be used. After the multi-level decomposition by l times, we get 2^l frequency bands with the same bandwidth defined according to equation (2).

$$[\frac{(i-l)f_n}{2}, \frac{if_n}{n}], \quad i = 1, 2, ..., 2^l, \quad (2)$$

where fn is the Nyquist frequency in the ith-frequency band. The mother wavelet decomposes the signal via low-pass filter $h(n)$ and $(2^l - 1)$ band-pass filters $g(n)$ to provide, at each level j, the full information in two frequency bands. A_j is the low-frequency approximation and D_j is the high-frequency detail signal [19]:

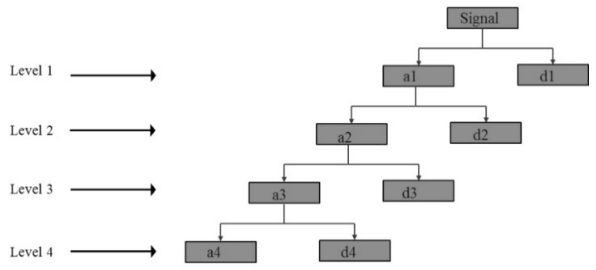

FIGURE 1. Wavelet tree decomposition.

$$\begin{cases} A_j(n) = \sum\limits_k h(k-2n)A_{j-1} \\ D_j(n) = \sum\limits_k g(k-2n)A_{j-1} \end{cases}, \; n = 0,1,2,3,..., \quad (3)$$

where $A_0(k)$ is the initial signal. After the multi-level decomposition, the approximation A_j and detail D_j signals will be generated for each node j.

The multi-level decomposition of the stator current was then achieved using the Daubechies *db*8 wavelet. When rotor eccentricity and load misalignment appear in the motor, the information about the fault in the stator current will be included in each frequency band generated by the DWT decomposition process.

The calculation of the vector energy for the approximations in each node allows the construction of a vector data which contain the necessary information about faults over a wide frequency band.

The approximations energy can be computed using the Euclidean norm (or 2-energy) of $A_i(n)$ that has N elements and is defined by:

$$\|EA_i\| = \frac{1}{N}\sqrt{\sum_{k=1}^{N} |A_i(k)|^2} \;, \; i = 1,2,.....N_{ls} \quad (4)$$

Figure 2 shows the estimation of the approximation's energy vector for each node and the corresponding frequency band.

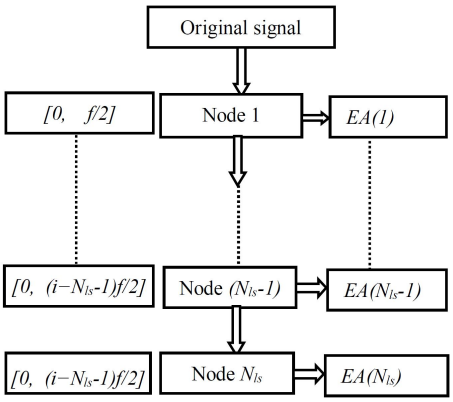

FIGURE 2. Approximations energy estimation steps.

The overall stator current analysis diagram is presented in Figure 3. The different steps are presented, from the stator current acquisition to the estimation of the energy for each level of decomposition.

3. FAULTS DESCRIPTION

In electrical machines, eccentricities are generally generated by the non-constant air-gap distribution. They are the most common faults in induction motors. According to recent studies, mechanical faults represent 50–60 % of the faults in electric motors. About 60 % of mechanical defects are linked to rotor eccentricities.

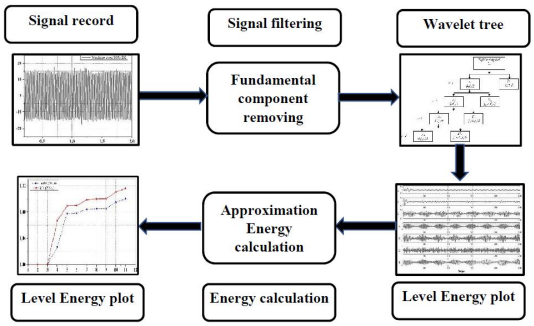

FIGURE 3. Stator current analysis steps.

Indeed, the rotor eccentricity is often generated from other defect such as bearing failures or load misalignments. The impact of this fault can be serious; this could even result in a breakdown of the motor due to rotor-to-stator friction [25–27].

Dynamic eccentricity (DE) take place when the rotor axle is not matching the rotation axle and the narrow side of the air-gap rotates at the same speed as the rotor (Figure 4). There are multiple causes of dynamic eccentricity and the most common are manufacturing tolerances, bearing wear, and incorrect manufacture of the machine components. Another source of dynamic eccentricity is the rotation of the rotors at a speed close to the critical speed; it is an important consideration in larger and flexible-shaft machines. In an induction machine, a dynamic eccentricity can be identified by examining the frequency components defined as follows [27–29]:

$$f_{de} = (1 \pm \frac{(1-s)}{p}) f_s, \quad (5)$$

where

f_de : the characteristic frequency of the DE

s : the Slip

f_s : the supply frequency

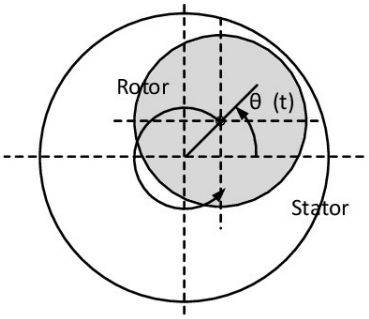

FIGURE 4. Dynamic eccentricity mechanism.

A non-constant air-gap generates a rotating radial force and an Unbalanced Magnetic Pull (UMP) on the rotor and stator due to the interaction of the space harmonic field components with pole pair numbers differing by one and rotating in the same direction.

The dynamic eccentricity may generate vibrations at the supply frequency and at the rotor frequency (f_r), these are given by $2f_r$, $2f_s \pm f_r$ [30]. where f_s is the supply frequency. A misalignment of the coupling is a condition in which the shaft of the drive machine and the driven machine are not on the same centre line (Figure 5). The misalignment can be parallel, angular or both (combined: parallel and angular). It is very difficult to obtain a perfect alignment between two shafts in industrial applications [28, 31].

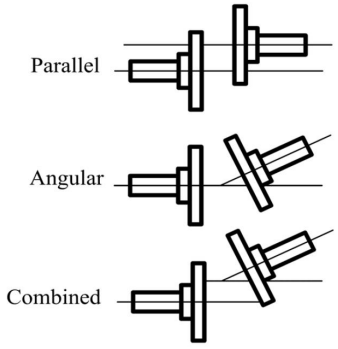

Figure 5. Shafts misalignment.

Even if a precise alignment is ensured, it cannot be maintained for a long time due to many external effects such as a disturbance of the base foundation. A shaft misalignment is a commonly encountered problem observed in the large rotor bearing machines and produces significant vibrations. Flexible couplings are commonly employed in industrial production chains to transmit mechanical power between the machine and the driven load. Most couplings transmit electromagnetic torque via an elastomer or a metal spring in order to reduce the vibration within an accepted level of misalignment. Electrical machines manufacturers suggest using the flexible couplings based on thermoplastics as active transmission elements for load aligning by using laser equipment or alignment clocks. The misaligned flexible couplings can transmit torque, producing high vibration levels and may cause damage to the shaft and bearings.

The misalignment induces harmonics in the stator current spectrum at frequencies, this makes it possible to detect these phenomena. However, since similar harmonics are produced by some mechanical faults, their detection and localisation are still a delicate matter when using MCSA. To overcome this limitation, it becomes necessary to identify misalignment faults over a wide band of frequency [4].

The main goal of this paper is to use the DWT approach for the detection of dynamic eccentricity and shaft misalignment in squirrel cage induction motors under various loading conditions, since the frequency components introduced by these faults depend on the load. Their detection and decision can constitute a powerful indicator for the diagnosis. In this work, the obtained approximation signals generated by the multilevel decomposition are used to build an energy vector calculated for each decomposition node. The method allows the detection based on the analysis of the energy of the signals that are amplified by the different faults. This method constitutes an important advantage when compared to the classical methods by analysing the stator current under a wide frequency band and avoiding the tracking of harmonics in a limited band or at predefined frequency.

Parameter	**Value**
Rated power	5.5 kW
Rated Voltage	400 V
Rated line current	10.5 A
Rated speed	1455 rpm
Rated power factor	0.88
DC motor	MS1321
Rated speed	1450 rpm
Rated power	3.9 kW
Rated Voltage	260 V
Rated current	17.6 A

Table 1. Characteristics of the 5.5 kW IM and DC load.

4. Experimental setup

An experimental analysis of the mechanical faults described previously has been carried out. The experimental setup contains a three-phase squirrel cage induction machine with 4 poles and a rated torque of 36 Nm. The induction motor is coupled to a DC motor to provide the necessary load. The used motors are driven by a variable speed drive (Leroy Somer) working in open loop. The DC motor is connected to a resistor bank via a DC-DC buck converter for controlling the armature current. The principal characteristics of tested machines are given in Table 1.

The experimental setup is illustrated in Figure 6. It consists mainly of an industrial induction motor with its drive loaded by a DC motor. Two induction motors with the same characteristics are tested. The first one is healthy; it will be considered as a reference for the comparison with the faulty one. The second motor is faulty and has a dynamic eccentricity and misalignment. The measurement card contains current sensors LA-55P, voltage sensors LV-25P, tachymeter and torque sensor. A maximum current and voltage of 50 A and 480 V can be achieved respectively.

The acquisition card used is a PCI data card, 16-bit, with a sampling frequency of 200 kHz, and it is installed in a computer and connected to the measuring board via a serial cable. These motors are supplied by the industrial drive and have been tested under three loading level conditions. All the experiments are carried out with the same sampling frequency 26,5 Hz during 10 s recording time. To obtain 50 % of DE, the original ball bearings are replaced by other ball bearings of the same external diameter, but of greater internal diameter. A 0.2 mm bore offset is introduced.

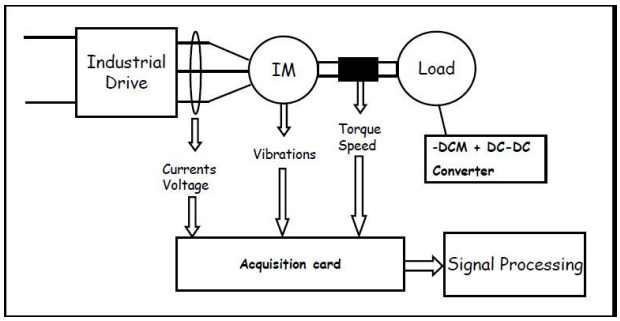

FIGURE 6. Mechanical faults experimental setup.

After an aligned positioning of the eccentric rings on the shaft (to guarantee a uniform direction of the eccentricity), we insert the new ball bearings. The introduced air-gap of the machine is considered to be 0.4 mm; 50 % of DE of the rotor compared to the stator (Figure 7).

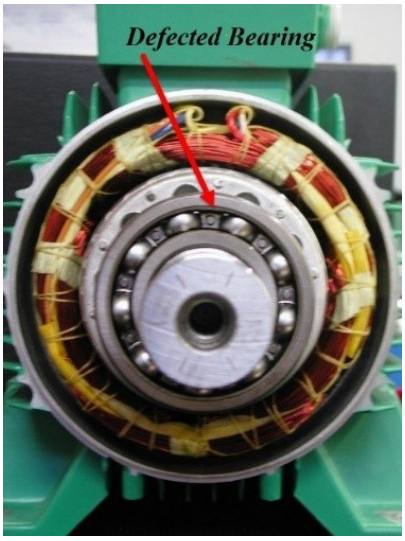

FIGURE 7. Eccentric bearing assembling.

The tests carried out to analyse the DE have been performed on two machines (a healthy machine and another with 50 % of DE) with the principal characteristics shown in Table 1. The sampling frequency of the measured signals was chosen equal to 25.6 KHz. The two machines were tested under three levels of load: 4 Nm, 18 Nm and 29 Nm of the nominal torque. The Figure 8 illustrates the wave form of the recorded stator current for the machine with the dynamic eccentricity.

In order to study a more realistic mechanical fault, a small misalignment of the load shaft is introduced under different loads (4 Nm, 18 Nm and 29 Nm). The Figure 9 shows the measurement of the misalignment degree.

For the misalignment faults, the same mechanical setup and signal processing steps as above are used for recording and analysing the stator current under the same loading conditions

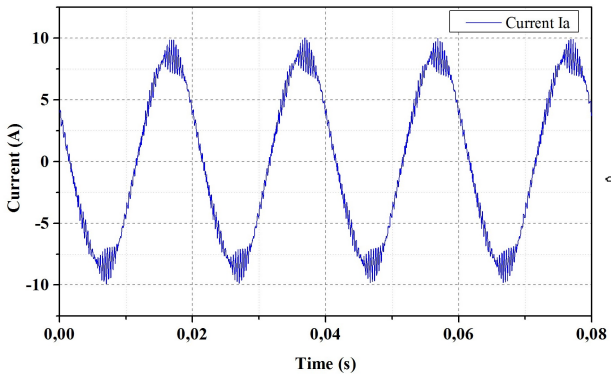

FIGURE 8. Recorded stator current with dynamic eccentricity.

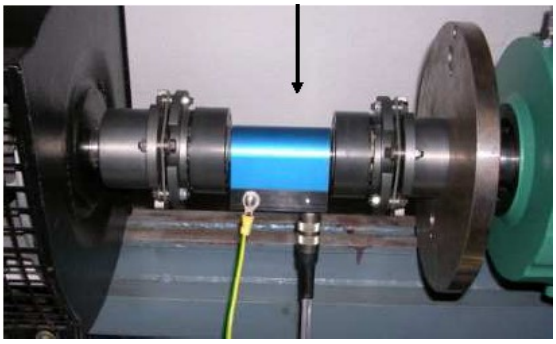

FIGURE 9. Misalignment degree measurement.

4.1. Stator current decomposition

The mother wavelets "db8" are used to decompose the stator current for each machine. The decomposition in multi-level requires some consideration in order to obtain a good approximation and detail signals.

4.2. Stator current filtering

Among the methods used in this paper, the fundamental component of the stator current has been removed before the signal goes through the multi-level decomposition process by DWT. This procedure amplifies the small harmonics induced by the faults.

4.3. Optimal level calculation

The required number of decompositions N_{ls} is linked to the acquisition conditions, such as the sampling frequency f and the supply frequency. The necessary level N_{ls} is chosen to obtain a high-level signal (approximation) with a highest frequency along which the faults harmonics are located. The minimum levels of decomposition needs an approximation signal (A_{nf}) with the upper limit of the frequency band being less than the fundamental frequency. This limit is expressed by the following condition [19].

$$2^{-(L_{ls}+1)} f_s < f \tag{6}$$

From this requirement, the successive decomposition of the approximation signals can be limited to level N_{ls} that is given by:

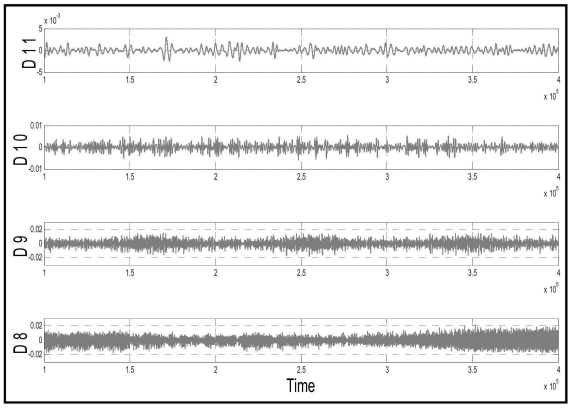

(A). Healthy motor.

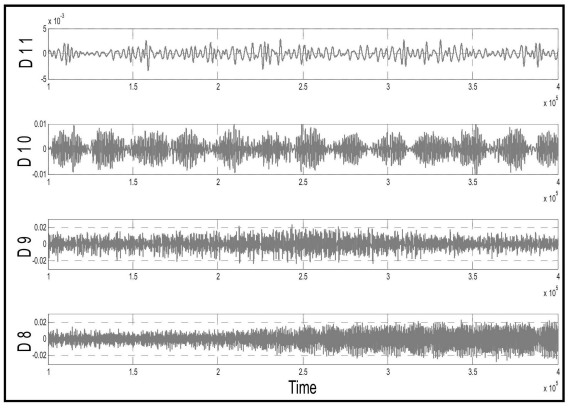

(B). Eccentric motor.

FIGURE 10. First 4 details signals for (A) symmetric motor and (B) eccentric motor.

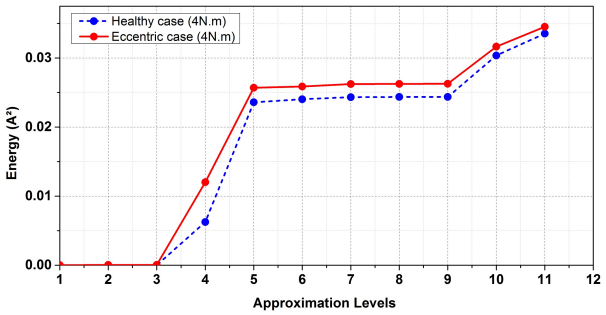

(A). 4 Nm

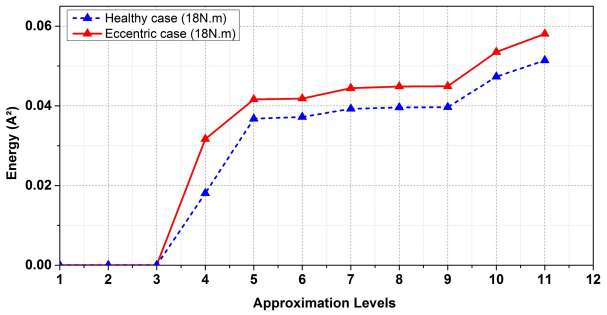

(B). 18 Nm

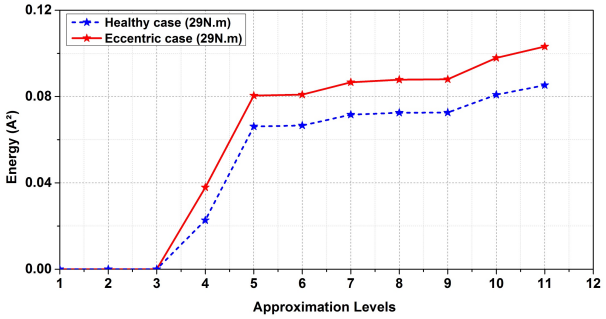

(C). 29 Nm

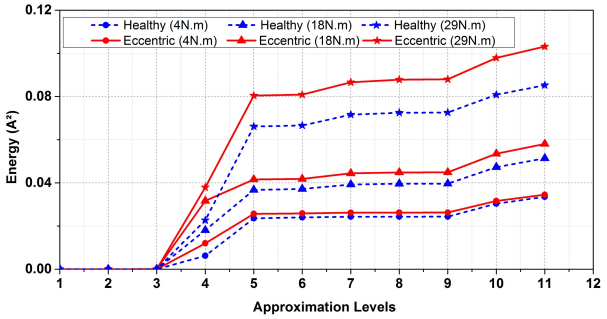

(D). all cases

FIGURE 11. Estimated nodes energy for eccentricity fault under (A) load = 4 Nm, (B) load = 18 Nm, (C) load = 29 Nm and (D) all cases.

$$N_{ls} = \text{int}\left(\frac{\log(f_s/f)}{\log(2)}\right). \tag{7}$$

For this technique, an additional decomposition of the stator current should be carried out so that the frequency band [0–f] is divided into several bands. Generally, two extra levels of decomposition $N_{ls} + 2$ will be suitable [19].

According to the suitable level, the different frequency bands are given in Table 2.

The Figure 10 compares the details obtained from DWT of a steady state stator current for a symmetric machine and for the eccentric machine with 50 $ of DE under a load 4 Nm. The purpose of this comparison is to demonstrate that when the harmonics are introduced by the dynamic eccentricity, the DWT analysis can distinguish clearly between the faults when present.

5. RESULTS AND DISCUSSION

5.1. DYNAMIC ECCENTRICITY

For the dynamic eccentricity fault, the energy vector is calculated for 11 levels with 3 loading levels. Figure 11 shows the plot of vector $\|EA_i\|$ for the three loading levels.

The analysis of the three figures shows an increase in energies for eccentric cases starting at level 3, which corresponds to the frequency band [0–3312.5Hz]. We also see that the deviation is important as a function

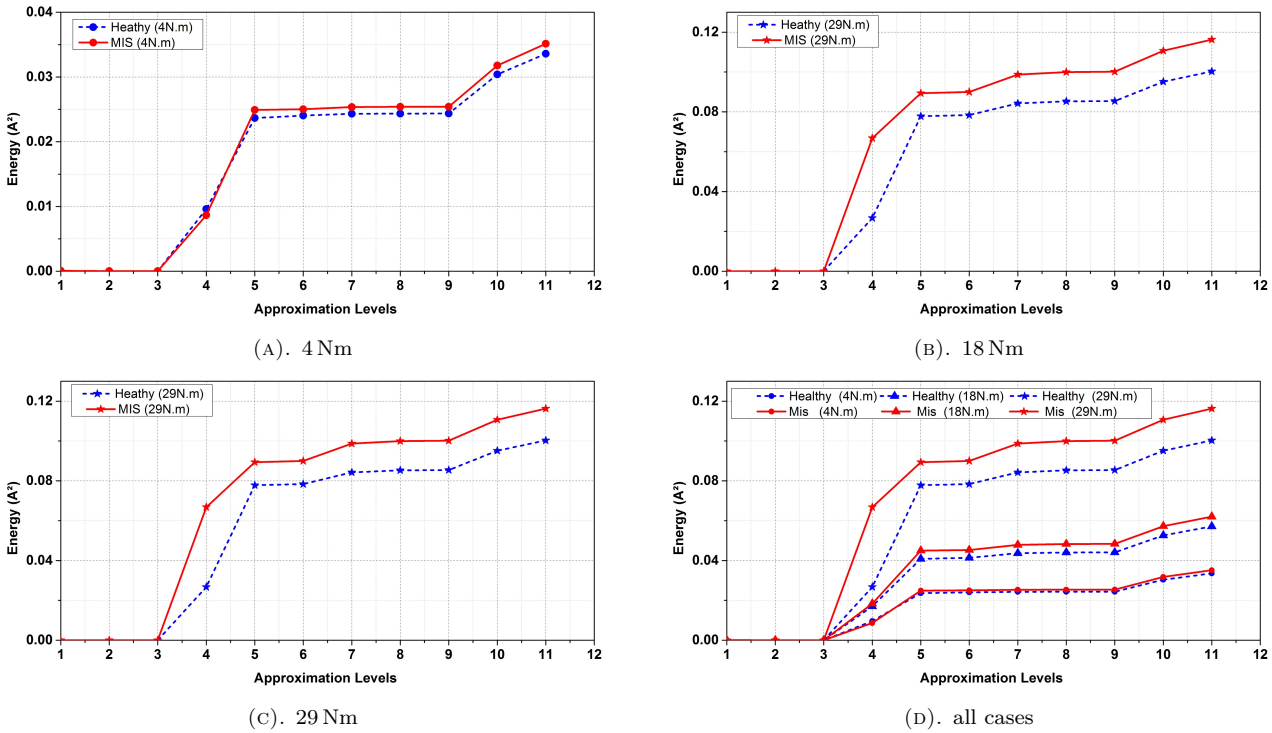

(A). 4 Nm (B). 18 Nm

(C). 29 Nm (D). all cases

FIGURE 12. Estimated nodes energy for misalignment fault under (A) load = 4 Nm, (B) load = 18 Nm, (C) load = 29 Nm and (D) all cases.

Level	A_i	**Band [Hz]**	D_i	**Band [Hz]**
J=1	A1	0-13250	D1	13250-26500
J=2	A2	0-6625	D2	6625-13250
J=3	A3	0-3312.5	D3	3312.5-6625
J=4	A4	0-1656.2	D4	1656.25-3312.5
J=5	A5	0-828.12	D5	828.12-1656.25
J=6	A6	0-414	D6	414-828.125
J=7	A7	0-207	D7	207-414
J=8	A8	0-103.5	D8	103.5-207
J=9	A9	0-51.75	D9	51.75-103.5
J=10	A10	0-25.87	D10	25.875-51.75
J=11	A11	0-12.94	D11	12.94-25.87

TABLE 2. Details and approximation bands for N_{ls}.

of the loading, even at high frequencies. These results show that eccentricity can be detected in the frequency band [0–4000 Hz] with useful information on the faults concentrated in the low frequencies and gradually decreasing in the high frequencies.

5.2. MISALIGNMENT

For the misalignment fault, the energy vector is also calculated for 11 levels with 3 loading levels. Figure 12 shows the plot of vector $\|EA_i\|$ for the three loading levels.

Similarly to the an eccentricity fault results, the figure analysis shows an increase in energies for misalignment cases beginning at level 3, which corresponds to the frequency band [0–3312.5 Hz].These results show that a misalignment fault can be detected in the frequency band [0–4000 Hz] with useful information concentrated in low frequencies and gradually decreasing in high frequencies. The curves obtained for mechanical faults show that the load has an important role in the detection process, and it is recommended to carry out the diagnostic operation under full loading conditions in order to increase the separation between the healthy and the defective machine.

A comparison between energies for healthy and defective machines under various loads is performed in order to show the energy deviation as a function of the load level. Table 3 displays numerical values for the energy deviation for various machine loadings. Figure 13 shows the graphical plot of this deviation for both cases of eccentric and misaligned machines.

The plot of the difference in energies of the nodes showed a large deviation when the load increases, precise for the fault of the dynamic eccentricity and less accurate for the fault of misalignment. This result is critical to consider when performing any diagnostic procedure. It is obvious that the diagnosis at high load is more precise than that at low load.

6. CONCLUSION

In this work, a study was carried out to diagnose electrical and mechanical faults under different loading levels in a squirrel cage induction machine. The main aim is to find an effective method to decide whether the machine is faulty or not. The proposed method is a multi-resolution analysis based on the Discrete Wavelet Transform (DWT). Unlike traditional methods based on the Fast Fourier Transform (FFT),

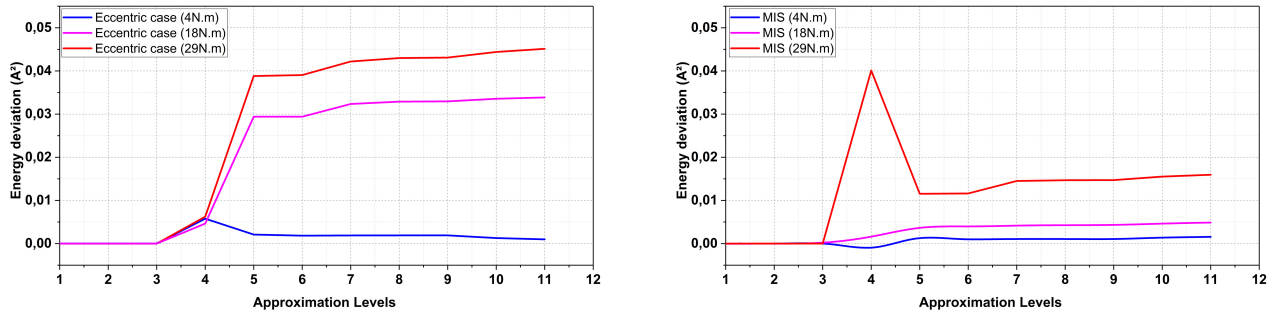

(A). Eccentric case.

(B). Misalignment case.

Figure 13. Energy deviation between healthy and faulty cases, (A) Eccentric case, (B) Misalignment case.

	Eccentric case			Misalignment case		
	4 Nm	18 Nm	29 Nm	4 Nm	18 Nm	29 Nm
Level 1	1.98E-05	-9.05E-06	-4.68E-06	6.09E-06	-2.99E-05	3.41E-06
Level 2	2.34E-05	-1.34E-05	-6.62E-06	4.49E-07	-1.81E-05	3.85E-06
Level 3	3.20E-05	-1.03E-05	-7.24E-06	4.20E-08	-1.66E-05	3.51E-06
Level 4	0.00578	0.00623	0.00464	-9.58E-04	0.00138	0.04011
Level 5	0.0021	0.03883	0.0294	0.00126	0.00416	0.01154
Level 6	0.00184	0.03904	0.0294	9.89E-04	0.00387	0.01162
Level 7	0.00189	0.04219	0.03235	0.00104	0.00421	0.01451
Level 8	0.0019	0.04299	0.03288	0.00105	0.00427	0.01469
Level 9	0.0019	0.04309	0.03295	0.00105	0.00427	0.01471
Level 10	0.00129	0.0444	0.03355	0.00137	0.00465	0.01553
Level 11	9.82E-04	0.04512	0.03386	1.55E-03	0.00487	0.01595

Table 3. Energy deviation between healthy and faulty machines.

the DWT method allows searching information for related to faults over wide frequency bands and to avoid tracking the fault indicators related to predefined frequencies. The results obtained by applying the proposed method on the different faults show the efficiency and the precision of detection and separation between healthy and defective machines. Moreover, the results show that the load applied during the acquisition process has an important role in the detection of mechanical faults.

We have also shown in this work that the diagnosis of faults at a high load is strongly recommended to reveal the different harmonics related to the fault. The proposed method in this paper also shows that the spectral content caused by the mechanical defects like eccentricity and misalignment is more important at high frequencies than at low frequencies.

References

[1] O. E. Hassan, M. Amer, A. K. Abdelsalam, B. W. Williams. Induction motor broken rotor bar fault detection techniques based on fault signature analysis – a review. *IET Electric Power Applications* **12**(7):895–907, 2018. https://doi.org/10.1049/iet-epa.2018.0054

[2] S. K. Ramu, G. C. R. Irudayaraj, S. Subramani, U. Subramaniam. Broken rotor bar fault detection using hilbert transform and neural networks applied to direct torque control of induction motor drive. *IET Power Electronics* **13**(15):3328–3338, 2020. https://doi.org/10.1049/iet-pel.2019.1543

[3] K. Gyftakis, P. Panagiotou, D. Spyrakis. Detection of simultaneous mechanical faults in 6 kV pumping induction motors using combined MCSA and stray flux methods. *IET Electric Power Applications* pp. 1–8, 2020 [E-First]. https://doi.org/10.1049/iet-epa.2020.0099

[4] H. S. Gerçekcıoğlu, M. Akar. Instantaneous power signature analysis for misalignment fault diagnosis in 3-phased induction motors. In *2018 26th Signal Processing and Communications Applications Conference (SIU)*, pp. 1–4. IEEE. https://doi.org/10.1109/SIU.2018.8404303

[5] R. A. Ayon-Sicaeros, E. Cabal-Yepez, L. M. Ledesma-Carrillo, G. Hernandez-Gomez. Broken-rotor-bar detection through STFT and windowing functions. In *2019 IEEE Sensors Applications Symposium (SAS)*, pp. 1–5. IEEE. https://doi.org/10.1109/SAS.2019.8706086

[6] P. Lombard, V. Fireteanu, A.-I. Constantin. Influences on the electromagnetic torque and rotor force of different faults in squirrel-cage induction motors. *International Journal of Applied Electromagnetics and Mechanics* **59**(3):805–815, 2019. https://doi.org/10.3233/jae-171136

[7] A. Kucuker, M. Bayrak. Detection of mechanical imbalances of induction motors with instantaneous power signature analysis. *Journal of Electrical Engineering and Technology* **8**(5):1116–1121, 2013. https://doi.org/10.5370/jeet.2013.8.5.1116

[8] W. T. Thomson. Vibration monitoring of induction motors and case histories on shaft misalignment and soft foot. In *Vibration Monitoring of Induction Motors*, pp. 1–46. Cambridge University Press, 2020. https://doi.org/10.1017/9781108784887.002

[9] T. Goktas, M. Arkan, M. S. Mamis, B. Akin. Separation of induction motor rotor faults and low frequency load oscillations through the radial leakage flux. In *2017 IEEE Energy Conversion Congress and Exposition (ECCE)*, pp. 3165–3170. IEEE, 2017. https://doi.org/10.1109/ecce.2017.8096576

[10] C. Prakash, R. K. Saini. IoT-based monitoring and controlling of crop field and induction motor protection from voltage fluctuation. *Agricultural Journal* **15**(4):49–56, 2020. https://doi.org/10.36478/aj.2020.49.56

[11] R. R. Schoen, T. G. Habetler. Evaluation and implementation of a system to eliminate arbitrary load effects in current-based monitoring of induction machines. In *IAS '96. Conference Record of the 1996 IEEE Industry Applications Conference Thirty-First IAS Annual Meeting*, vol. 1, pp. 671–678. IEEE. https://doi.org/10.1109/ias.1996.557108

[12] M. Singh, A. G. Shaik. Broken rotor bar fault diagnosis of a three-phase induction motor using discrete wavelet transform. In *2019 IEEE PES GTD Grand International Conference and Exposition Asia (GTD Asia)*, pp. 13–17. IEEE, 2019. https://doi.org/10.1109/gtdasia.2019.8715925

[13] O. Bolshunova, A. Kamyshian, A. Bolshunov. Diagnostics of career dump truck traction induction motors technical condition using wavelet analysis. In *2016 Dynamics of Systems, Mechanisms and Machines (Dynamics)*, pp. 1–4. IEEE. https://doi.org/10.1109/Dynamics.2016.7818988

[14] M. Z. Ali, M. N. S. K. Shabbir, S. M. K. Zaman, X. Liang. Single- and multi-fault diagnosis using machine learning for variable frequency drive-fed induction motors. *IEEE Transactions on Industry Applications* **56**(3):2324–2337, 2020. https://doi.org/10.1109/tia.2020.2974151

[15] M. Z. Ali, M. N. S. K. Shabbir, X. Liang, et al. Machine learning-based fault diagnosis for single- and multi-faults in induction motors using measured stator currents and vibration signals. *IEEE Transactions on Industry Applications* **55**(3):2378–2391, 2019. https://doi.org/10.1109/tia.2019.2895797

[16] F. Wu, Y. Hao, J. Zhao, Y. Liu. Current similarity based open-circuit fault diagnosis for induction motor drives with discrete wavelet transform. *Microelectronics Reliability* **75**:309–316, 2017. https://doi.org/10.1016/j.microrel.2017.05.036

[17] T. K. Sarkar, C. Su, R. Adve, et al. A tutorial on wavelets from an electrical engineering perspective. I. Discrete wavelet techniques. *IEEE Antennas and Propagation Magazine* **40**(5):49–68, 1998. https://doi.org/10.1109/74.735965

[18] B. A. Vinayak, K. A. Anand, G. Jagadanand. Wavelet-based real-time stator fault detection of inverter-fed induction motor. *IET Electric Power Applications* **14**(1):82–90, 2020. https://doi.org/10.1049/iet-epa.2019.0273

[19] A. Bouzida, O. Touhami, R. Ibtiouen, et al. Fault diagnosis in industrial induction machines through discrete wavelet transform. *IEEE Transactions on Industrial Electronics* **58**(9):4385–4395, 2010. https://doi.org/10.1109/TIE.2010.2095391

[20] T. Ameid, A. Menacer, H. Talhaoui, Y. Azzoug. Discrete wavelet transform and energy eigen value for rotor bars fault detection in variable speed field-oriented control of induction motor drive. *ISA Transactions* **79**:217–231, 2018. https://doi.org/10.1016/j.isatra.2018.04.019

[21] N. R. Alham, R. M. Utomo, D. A. Asfani, et al. Detection of unbalanced voltage supply and static eccentricity on three-phase induction motor using discrete wavelet transform. In *2020 12th International Conference on Information Technology and Electrical Engineering (ICITEE)*, pp. 269–274. IEEE. https://doi.org/10.1109/ICITEE49829.2020.9271691

[22] M. A. Mohamed, A.-A. A. Mohamed, M. Abdel-Nasser, et al. Induction motor broken rotor bar faults diagnosis using ANFIS-based DWT. *International Journal of Modelling and Simulation* **41**(3):220–233, 2021. https://doi.org/10.1080/02286203.2019.1708173

[23] B. Belkacemi, S. Saad, Z. Ghemari, et al. Detection of induction motor improper bearing lubrication by discrete wavelet transforms (DWT) decomposition. *Instrumentation Mesure Métrolo* **19**(5):347–354, 2020. https://doi.org/10.18280/i2m.190504

[24] I. Chouidira, D. Khodja, S. Chakroune. Continuous wavelet technique for detection of broken bar faults in induction machine. *Traitement du Signal* **36**(2):171–176, 2019. https://doi.org/10.18280/ts.360207

[25] K. Tian, T. Zhang, Y. Ai, W. Zhang. Induction motors dynamic eccentricity fault diagnosis based on the combined use of WPD and EMD-simulation study. *Applied Sciences* **8**(10):1709, 2018. https://doi.org/10.3390/app8101709

[26] Nikhil, L. Mathew, A. Sharma. Various indices for diagnosis of air-gap eccentricity fault in induction motor – a review. *IOP Conference Series: Materials Science and Engineering* **331**:012032, 2018. https://doi.org/10.1088/1757-899x/331/1/012032

[27] G. Mirzaeva, K. I. Saad. Advanced diagnosis of rotor faults and eccentricity in induction motors based on internal flux measurement. *IEEE Transactions on Industry Applications* **54**(3):2981–2991, 2018. https://doi.org/10.1109/TIA.2018.2805730

[28] A. Ortiz, J. Garrido, Q. Hernandez-Escobedo, B. Escobedo-Trujillo. Detection of misalignment in motor via transient current signature analysis. In *2019 IEEE International Conference on Engineering Veracruz (ICEV)*, vol. 1, pp. 1–5. IEEE. https://doi.org/10.1109/ICEV.2019.8920719

[29] A. F. Aimer, A. H. Boudinar, M. E. A. Khodja, et al. Monitoring and fault diagnosis of induction motors mechanical faults using a modified auto-regressive approach. In *Advanced Control Engineering Methods in Electrical Engineering Systems*, pp. 390–410. Springer International Publishing, 2018. https://doi.org/10.1007/978-3-319-97816-1_30

[30] R. S. C. Pal, A. R. Mohanty. A simplified dynamical model of mixed eccentricity fault in a three-phase induction motor. *IEEE Transactions on Industrial Electronics* **68**(5):4341–4350, 2020. https://doi.org/10.1109/TIE.2020.2987274

[31] S. Prainetr, S. Tunyasrirut, S. Wangnipparnto. Testing and analysis fault of induction motor for case study misalignment installation using current signal with energy coefficient. *World Electric Vehicle Journal* **12**(1):37, 2021. https://doi.org/10.3390/wevj12010037